Vaughn, J. C., Sperbeck, S. J., Ramsey, W. J., & Lawrence, C. B. (1984) *Nucleic Acids Res. 12*, 7479–7502.
Vigne, R., Jordan, B. R., & Monier, R. (1973) *J. Mol. Biol. 76*, 303–311.
Woese, E. R., Magrum, L. J., Gupta, R., Siegel, R. B., & Stahl, D. A. (1980) *Nucleic Acids Res. 8*, 2275–2293.
Wong, Y. P., Kearns, D. R., Reid, B. R., & Shulman, R. G. (1972) *J. Mol. Biol. 72*, 741–749.
Wrede, P., & Erdmann, V. A. (1973) *FEBS Lett. 33*, 315–319.
Zagorska, L., Duin, J. V., Noller, H. F., Pace, B., Johnson, K. D., & Pace, N. R. (1984) *J. Biol. Chem. 259*, 2798–2802.

Binding of *Escherichia coli* Protein Synthesis Initiation Factor IF1 to 30S Ribosomal Subunits Measured by Fluorescence Polarization†

Frank H. Zucker‡ and John W. B. Hershey*
Department of Biological Chemistry, School of Medicine, University of California, Davis, California 95616
Received September 17, 1985; Revised Manuscript Received February 5, 1986

ABSTRACT: The interaction of initiation factor IF1 with 30S ribosomal subunits was measured quantitatively by fluorescence polarization. Purified IF1 was treated with 2-iminothiolane and *N*-[[(iodoacetyl)amino]ethyl]-5-naphthylamine-1-sulfonic acid in order to prepare a covalent fluorescent derivative without eliminating positive charges on the protein required for biochemical activity. The fluorescent-labeled IF1 binds to 30S subunits and promotes the formation of *N*-formylmethionyl-tRNA complexes with 70S ribosomes. Analyses of mixtures of fluorescent-labeled IF1 and 30S ribosomal subunits with an SLM 4800 spectrofluorometer showed little change in fluorescence spectra or lifetimes upon binding, but a difference in polarization between free and bound forms is measurable. Bound to free ratios were calculated from polarization data and used in Scatchard plots to determine equilibrium binding constants and number of binding sites per ribosomal subunit. Competition between derivatized and nonderivatized forms of IF1 was quantified, and association constants for the native factor were determined: $(5 \pm 1) \times 10^5$ M^{-1} with IF1 alone; $(3.6 \pm 0.4) \times 10^7$ M^{-1} with IF3; $(1.1 \pm 0.2) \times 10^8$ M^{-1} with IF2; $(2.5 \pm 0.5) \times 10^8$ M^{-1} with both IF2 and IF3. In all cases, 0.9–1.1 binding sites per 30S subunit were detected. Divalent cations have little effect on affinities, whereas increasing monovalent cations inhibit binding. On the basis of the association constants, we predict that greater than 90% of native 30S subunits are complexed with all three initiation factors in intact bacterial cells.

During initiation of protein synthesis in bacteria, the 70S ribosome dissociates into subunits, the 30S subunit forms a preinitiation complex with *N*-formylmethionyl-tRNA ($fMet\text{-}tRNA_f$)[1] and mRNA, and the 50S subunit joins the preinitiaton complex to form a 70S initiation complex capable of entering the elongation phase [for reviews, see Maitra et al. (1982) and Grunberg-Manago et al. (1978)]. This process is promoted by three initiation factors: IF1 (M_r 8119), IF2 (M_r 97 300 and 79 700) and IF3 (M_r 20 668). IF3 helps dissociate ribosomes and is associated with mRNA binding. IF2 is involved with fMet-tRNA binding and hydrolyzes GTP. IF1 stimulates the rate of ribosome dissociation and generally assists in the actions of the other two factors. In spite of extensive efforts over the past 15 years, the detailed molecular mechanisms of action of the initiation factors remain unclear.

Elucidation of the pathway of initiation and of possible translational control mechanisms requires a detailed knowledge of the kinetic parameters for the various reactions involved. Studies of the rates of binding of fMet-tRNA and mRNA by membrane filtration (Gualerzi et al., 1977; van der Hofstad et al., 1978) and spectrophotometric (Wintermeyer & Gualerzi, 1983) techniques indicate that their binding may be either a random or an ordered process. We have focused on the interaction of the initiation factors with 30S subunits, initially using radiolabeled factors and sucrose density gradient centrifugation to monitor binding (Fakunding & Hershey, 1973; Heimark et al., 1976; Langberg et al., 1977). Whereas these studies showed that individually the stability of 30S binding is IF3 > IF2 > IF1, this method is unsuited to quantitative kinetic studies. More recently we used fluorescence polarization techniques to determine the equilibrium association constants (K_a) for 30S subunits and IF2 (Weiel & Hershey, 1982) and IF3 (Weiel & Hershey, 1981). Fluorescence polarization allows measurement of the binding of a small, covalently derivatized initiation factor with the relatively large 30S ribosomal subunit. The K_a for IF3 and 30S subunits is 3.1×10^7 M^{-1} and does not change appreciably in the presence of the other factors. The K_a for IF2 alone is 2.7×10^7 M^{-1} but increases to 1.8×10^8 M^{-1} in the presence of IF1 and IF3. In the work reported here, we prepared an active fluorescent derivative of IF1 and measured the K_a for IF1 and 30S subunits with and without the other factors. The

†This research was supported by Grant NP-70 from the American Cancer Society.
‡Present address: Fred Hutchinson Cancer Research Center, Seattle, WA 98104.

[1] Abbreviations: fMet-tRNA, *N*-formylmethionyl-tRNA; IF, initiation factor; PAGE, polyacrylamide gel electrophoresis; SDS, sodium dodecyl sulfate; NEPHGE, nonequilibrium pH gradient electrophoresis; BME, β-mercaptoethanol; TEA, triethanolamine; 2-ITL, 2-iminothiolane; F-IF1, fluorescent-labeled IF1; 1,5-IAEDANS, *N*-[[(iodoacetyl)amino]ethyl]-5-naphthylamine-1-sulfonic acid; Tris-HCl, tris(hydroxymethyl)aminomethane hydrochloride; EDTA, ethylenediaminetetraacetic acid.

0006-2960/86/0425-3682$01.50/0

combined results for the three factors begin to provide a quantitative analysis of this complex system.

Materials and Methods

1,5-IAEDANS (Hudson & Weber, 1973) was from Polysciences Inc.; acrylamide and triethanolamine were from Kodak; phosphocellulose P-11 was from Whatman; Sephadex G-50, DEAE-Sephadex, and course Sephadex G-25 were from Pharmacia. Initiation factors were purified from *Escherichia coli* MRE 600 as previously described (Hershey et al., 1977) and were greater than 95% pure as judged by PAGE in SDS buffer. The 30S subunits were prepared from tightly coupled 70S ribosomes by centrifugation at high pressure (47 500 rpm in a Beckman TI-14 rotor) and low magnesium (2 mM free Mg^{2+}) to separate 30S and 50S subunits in a hyperbolic sucrose gradient (Weiel & Hershey, 1981). Subunits were stored in small aliquots in liquid nitrogen, thawed, and used that day only. The 30S subunits were activated before use by heating at 40 °C for 15–20 min in 50 mM Tris-HCl, pH 7.6, 20 mM $Mg(OAc)_2$, 200 mM NH_4Cl, and 2 mM dithioerythritol (Zamir et al., 1971).

Buffer A contained 10 mM potassium phosphate, pH 7.5, 0.1 mM EDTA; 7 mM β-mercaptoethanol (BME); 5% glycerol, and KCl as indicated in millimoles per liter in parentheses. Buffer B contained 10 mM Tris-HCl, pH 7.6, 7 mM BME, and total monovalent salt (KCl + NH_4Cl) and $Mg(OAc)_2$ as indicated in parentheses. Buffers for fluorescent modification contained mixtures of TEA adjusted to pH 8.0 with HCl, and TEA free base, at the concentrations and proportions indicated.

General Methods. Protein concentrations were determined by the method of Schaffner and Weissmann (1973). SDS/PAGE was run according to the technique of Maizel (1971) and Laemmli (1970). Nonequilibrium pH gradient electrophoresis (NEPHGE) in 10% acrylamide gels was essentially as described by O'Farrell et al. (1977) for the first dimension.

Fluorescent Derivatization of IF1. 2-Iminothiolane (2-ITL) hydrochloride (Pierce Chemical Co.) (132 nmol) was freshly dissolved in 8.2 μL of 500 mM triethanolamine (TEA) free base and 8.2 μL of 500 mM TEA-HCl, pH 8.0. A solution of 1,5-IAEDANS (132 nmol) in 163 μL of 10 mM TEA-HCl, pH 8, was added, followed immediately by highly purified IF1 (0.9 mg; 111 nmol) in 163 μL of buffer A (600). The mixture was stirred for 24 h at 4 °C in the dark. The reaction was stopped by adding 5 μL of 0.25 M glycinamide and 0.25 M BME (about a 10-fold excess over 2-ITL and 1,5-IAEDANS). IF1 and its derivatives were separated from low molecular weight reagents on a coarse Sephadex G-25 column (0.6 cm × 22 cm) pretreated with 1 mL of a mixture containing 4 mg of lysozyme, 0.8 mM 1,5-IAEDENS, and 0.8 mM 2-ITL in 50 mM TEA and 50 mM TEA-HCl, pH 8.0. The stopped F-IF1 reaction mixture was loaded onto the column with 16-cm hydrostatic pressure and eluted with buffer A (0) at 0.12 mL/min into 0.5-mL fractions. The column fractions were monitored for protein concentration and fluorescence intensity, and the early eluting protein and fluorescent peak (fractions 6 and 7) contained about 90% of the recovered protein and was well separated from later eluting fluorescent material. F-IF1 derivatives were recovered in about 40% overall yield.

Fluorescence Measurements. Fluorescence intensity, polarization, and lifetime were measured on an SLM 4800 spectrofluorometer (SLM/Aminco) equipped with single diffraction monochromators, radio-frequency modulation tank, and Glan-Thompson polarizers. Data was collected and analyzed on an HP 9825A computer and an HP 9826A plotter (Hewlett-Packard). Polarization was measured in the T configuration with the excitation polarizer in the stem and the vertical and horizontal analyzers in the two arms. Excitation was at 337 ± 8 nm, and emission was measured through matched 470- or 500-nm cutoff filters (Schott) in both arms of the T.

F-IF1 titrations were run at several fixed 30S concentrations for each combination of IF2 and IF3. Cuvettes were presoaked in a solution of bovine serum albumin (BSA) and lysozyme (roughly 0.3 mg/mL each), to limit protein loss on cell walls, and then rinsed in buffer. Except where noted, samples contained buffer B (100, 5), heat-activated 30S subunits, and IF2 and IF3 at 300 nM excess over 30S subunits. Before F-IF1 was added, the offsets on the instrument were adjusted to give zero readings for vertical and horizontal emission from horizontal excitation, and then vertical and horizontal scatterings from this blank were measured with vertical excitation (V_b and H_b). F-IF1 was then titrated into the sample to raise the F-IF1:30S ratio from 0.25 to 3 or 4, without significantly altering the 30S concentration. For concentrations of 30S subunits under 1 μM, 2–30 μL of F-IF1 in buffer B (100, 5) was added to 1-mL samples in a 10 mm × 10 mm cuvette. To conserve material at higher concentrations, F-IF1 was diluted in buffer B (100, 5) with 30S subunits, IF2, and IF3 as in the blank; 2–50 μL of this F-IF1 solution was added to 0.1-mL samples in a 3 mm × 3 mm cuvette.

Polarization was determined after each addition of fluorescent factor in a modification of the procedure described by (Weiel & Hershey, 1981, 1982). Fifty single measurements (0.25 s each) were collected for each of three values: V = vertical excitation, vertical emission; H = vertical excitation, horizontal emission; correction factor C, the ratio of vertical to horizontal emission with horizontally polarized excitation. Polarizations were calculated from averages of these sets of 50 readings:

$$P = \frac{(V - V_b)/C - (H - H_b)}{(V - V_b)/C + (H - H_b)}$$

Measurements were repeated until P was stable, i.e., until there was no consistent drift. Then further readings (generally 10 or more) were taken, and a weighted average of these P's was calculated.

Polarization Data Analysis. Linear regression procedures (Worthing & Geffner, 1949) were modified for variable errors in both x and y directions using successive approximations to find the least-squares fit. The ratio of bound to free F-IF1 (F_b/F_f) was computed from observed polarization P by

$$\frac{F_b}{F_f} = \frac{Q_f}{Q_b}\frac{(P - P_f)}{(P_b - P)} \quad (1)$$

where Q_f/Q_b (the ratio of free to bound quantum yield) was determined from spectral data and from intensity measurements during F-IF1 titrations. Polarizations for free and bound F-IF1 (P_f and P_b) were determined as previously described (Weiel & Hershey, 1981; Dandliker et al., 1964). The amount of F-IF1 bound to 30S (F_b) was determined from this bound to free ratio and M, the amount of F-IF1 added:

$$F_b = M\frac{F_b/F_f}{F_b/F_f + 1} \quad (2)$$

Native IF1 is present in the F-IF1 preparation due to incomplete derivatization, so the standard Scatchard plot (Scatchard, 1949) was modified. Assuming IF1 and F-IF1 have the same maximum number of binding sites, the equilibrium equations are

for nonderivatized IF1

$$K_{an} = \frac{N_b}{N_f(nR - N_b - F_b)} \quad (3a)$$

for fluorescent-labeled IF1

$$K_{af} = \frac{F_b}{F_f(nR - N_b - F_b)} \quad (3b)$$

where R is the concentration of ribosomal subunits, n is the number of sites per subunit, and N_b is the amount of nonderivatized IF1 bound. From eq 3b

$$F_b/F_f = K_{af}nR - K_{af}(F_b + N_b) \quad (4)$$

Model 1. If derivatization did not change IF1's affinity constant ($K_{an} = K_{af}$), then the ratio of bound IF1 to total IF1 (W) would be the same as that of bound F-IF1 to total F-IF1, so $N_b = F_b(W/M)$. Substituting this into eq 4 gives

$$F_b/F_f = K_{af}nR - K_{af}F_b(1 + W/M) \quad (5a)$$

and dividing by R

$$(F_b/F_f)/R = K_{af}n - K_{af}(F_b/R)(T/M) \quad (5b)$$

where T is the total amount of IF1 derivatives added ($M + W$). A plot of $(F_b/F_f)/R$ vs. $(F_b/R)(T/M)$ should thus give a straight line as on a standard Scatchard plot, with a slope of $-K_{af} = -K_{an}$ and an intercept on the x axis of n.

Model 2. If derivatization perturbs F-IF1 binding ($K_{af} \neq K_{an}$), then N_b can be estimated by dividing eq 3a by eq 3b, solving for N_b/N_f

$$\frac{N_b}{N_f} = \frac{F_b}{F_f}\frac{K_{an}}{K_{af}} \quad (6)$$

and using this ratio analogously to eq 2:

$$N_b = \frac{W(N_b/N_f)}{N_b/N_f + 1} = W\frac{F_b/F_f}{F_b/F_f + K_{af}/K_{an}}$$

Dividing by eq 2 and multiplying both sides by F_b give an estimate of N_b on the basis of K_{af}/K_{an} and W/M:

$$N_b = F_b\frac{W(F_b/F_f + 1)}{M(F_b/F_f + K_{af}/K_{an})} \quad (7)$$

Substituting this N_b into eq 4 gives

$$F_b/F_f = K_{af}nR - K_fF_b\left[1 + \frac{W(F_b/F_f + 1)}{M(F_b/F_f + K_{af}/K_{an})}\right] \quad (8)$$

This differs from eq 5a only by the factor multiplying W/M on the right. At high F_b/F_f, this factor approaches 1 and the curve of $(F_b/F_f/R$ vs. $(F_b/R)(T/M)$ approaches the straight line expected if $K_{af} = K_{an}$; thus, the upper points (low F-IF1 concentrations) were used to determine K_{af} and n. As excess F-IF1 and IF1 were added, the extent of deviation from the expected line was used to quantify K_{af}/K_{an}, a measure of the perturbation caused by derivatization. IF1 binding for the lower points (high F-IF1 concentrations) was calculated from the K_{af} estimated from upper points. Solving eq 3b for N_b

$$N_b = nR - (F_b/F_f)/K_{af} - F_b \quad (9)$$

This estimate of N_b was used to calculate N_b/N_f, which was plotted vs. F_b/F_f according to eq 6 to give a line through the origin with a slope of K_{af}/K_{an}. This ratio was then used to calculate K_{an} from K_{af}.

Two methods were used to evaluate the affinity constants and stoichiometries thus determined. The residual error (RE) was computed from the square root of the weighted average of the squared distance between points observed and predicted from F_b/F_f by solving eq 8 for F_b. The validity of initial values

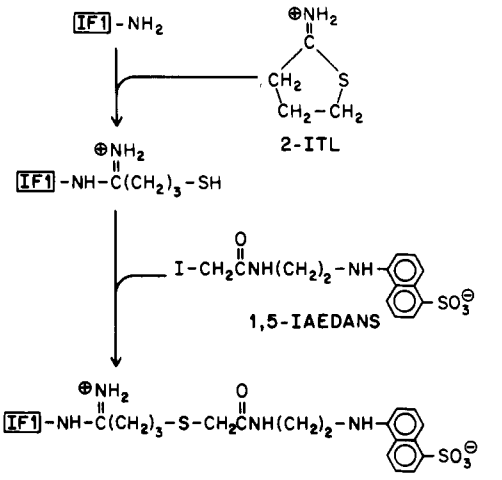

FIGURE 1: Synthesis of fluorescent IF1.

was confirmed by cyclic approximation: the "bound" axis was adjusted by using K_{af}/K_{an} according to eq 8, and a new K_{af} was determined from this corrected Scatchard plot using all points. N_b was then recalculated from the new K_{af} and used to estimate K_{af}/K_{an}, which could then be used for another correction cycle.

Lifetime Measurements. The excitation beam was modulated by refraction through 19% ethanol in H_2O oscillating in standing waves at 5.97, 17.911, or 29.853 MHz (referred to as 6, 18, or 30 MHz). Lifetimes were calculated from the average of 10–20 sets of 10 single measurements of fluorescence demodulation and phase delay (Spencer & Weber, 1967). Samples were 0.4 μM free F-IF1, 0.4 μM F-IF1 with 1 μM 30S subunits, 1.5 μM IF2, and 1.5 μM IF3 [both in 1 mL of buffer B (100, 5) in 10 mm × 10 mm cuvettes], and 0.5 μM F-IF1 with 4 μM 30S [in 0.1 mL of buffer B (100, 5) in a 3 mm × 3 mm cuvette]. For each sample, lifetimes were estimated from phase (τ_m) at all three frequencies. Calculated τ_p and τ_m from pairs of frequencies were used to resolve heterogeneous components (Weber, 1981), and components were fit to data from all three frequencies at once by a parabolic approximation least-squares search.

RESULTS

Preparation of Fluorescent-Labeled IF1 (F-IF1). In studying the interactions of IF1 with ribosomes, the use of the intrinsic fluorescence of IF1 is impractical because of contributions by the much larger amounts of protein in the ribosome. We therefore needed to prepare a covalent fluorescent derivative of IF1 whose absorption spectrum does not overlap that of the ribosome. In addition, the derivatization reaction should not greatly alter the activity of the factor. In previous work, we found that acylation of apparently any one of the lysine ε-amino groups or the N-terminal α-amino group is sufficient to inactivate IF1 (J. Kolberg and J. Hershey, unpublished results). Furthermore, the protein lacks a cysteine residue, nor can the two tyrosines act as targets since modification of either one destroys activity (Gualerzi & Pon, 1981). We therefore chose to treat IF1 with 2-iminothiolane (2-ITL), which converts an amino group to an amidino group, thus preserving its positive charge, and generates a free sulfhydryl group. The strongly fluorescent aminonaphthylsulfonate group can be attached by treating the sulfhydryl group with 1,5-IAEDANS. These reactions are shown in Figure 1.

Highly purified IF1 (greater than 97% pure) was treated with a small molar excess of 2-ITL and 1,5-IAEDANS as described under Materials and Methods. Pilot reactions were run to empirically determine the concentrations of reagents

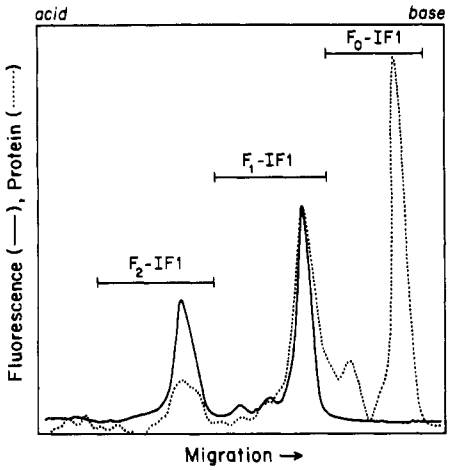

FIGURE 2: NEPHGE analysis of F-IF1 derivatization. The F-IF1 preparation described in the text was subjected to nonequilibrium pH gradient electrophoresis in 10% polyacrylamide slab gels (100 × 150 mm) with migration from acid to base (left to right in figure). The gel was illuminated with UV light and photographed through a 500-nm cutoff filter. Subsequently, the gel was fixed in 20% TCA, stained with 0.04% Coomassie Blue R250 (Pierce), 0.05% Crocein Scarlet (Sigma), 0.5% $CuSO_4$ in 27% ethanol, 10% acetic acid, and destained in 0.5% $CuSO_4$ in 12% ethanol–7% acetic acid. The negative and the stained gel were scanned with a Cary 210 spectrophotometer (Matthews, 1984) to record fluorescence intensity (—) and protein (···). Fluorescence and protein signals are on arbitrary scales adjusted to match the height of the major F_1-IF1 peak. The relative areas under major protein peaks and minor peaks to their left are the following: F_0-IF1, 52 ± 3% of the total; F_1-IF1, 37 ± 3%; F_2-IF1, 10 ± 2%; F_3-IF1 and higher derivatives, 1 ± 4%.

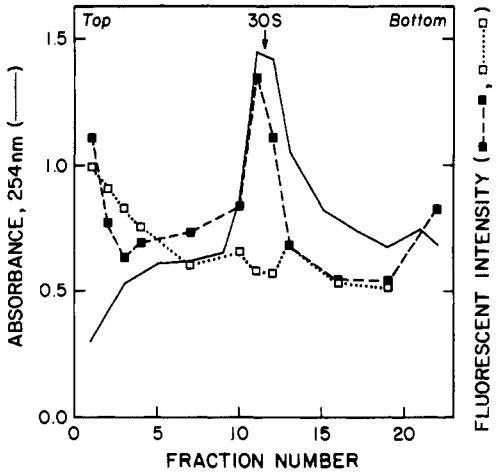

FIGURE 3: Sucrose gradient analysis of F-IF1 binding to 30S subunits. Mixtures of 75 pmol of 30S subunits and 75 pmol of F-IF1 with or without 150 pmol of IF2 and 150 pmol of IF3 were incubated 15 min at 30 °C in 0.11 mL of buffer B (100, 5) and centrifuged in 5–20% sucrose gradients as previously described (Langberg et al., 1977). Fractions (0.2 mL) were analyzed for absorption at 254 nm and for fluorescent intensity with 337-nm excitation, 16-nm slit width, and 470-nm emission filters: samples with IF2 and IF3 (■); samples without IF2 and IF3 (□).

and reaction time required to give about one dansyl group per IF1 molecule. This level of derivatization should result in the attachment of label to a large fraction of the molecules but minimize highly labeled factors which may be less active. The extent of reaction was followed by PAGE as will be described. Under the conditions used, the reaction with 2-ITL is rate limiting, whereas 1,5-IAEDANS reacts with the generated sulfhydryl groups relatively rapidly. The F-IF1 products subsequently were separated from reagents by passage through a Sephadex G-25 column as described under Materials and Methods. That the F-IF1 preparation contains dye covalently linked to protein was shown by PAGE in SDS buffers, where the fluorescence comigrated with the factor (results not shown).

Characterization of F-IF1. In order to determine the number of fluorescent probes added to IF1, the F-IF1 preparation was subjected to NEPHGE in 10% polyacrylamide gels as shown in Figure 2. Such gels separate the various derivatives of IF1 according to the number of probes added, by taking advantage of the negative sulfonate group on the naphthyl rings. The fastest migrating (most basic) molecule is nonderivatized IF1 (F_0–IF1), which is detectable by protein staining but shows no fluorescence. Monoderivatized IF1 (F_1-IF1) migrates more slowly and shows both fluorescence and protein staining. Lesser amounts of F_2-IF1 are seen and little or no F_3-IF1 is detected. The ratio of fluorescence to protein stain in F_2-IF1 is about twice that seen for F_1-IF1, as expected. The minor amount of protein staining material found between F_0-IF1 and F_1-IF1 is presumably due to derivatization of IF1 by 2-ITL, since such material is undetected in nontreated samples of IF1, but no attempt was made to further characterize the minor forms. The sum of F_0-IF1 and the minor nonfluorescent material is 52% of the protein. F_1-IF1 corresponds to 37%, F_2-IF2 to 10%, and higher derivatives to 1% of the protein. Therefore, on the average there are 0.6 fluorescent probe per IF1 molecule in this preparation, a value in reasonable agreement with the value of 0.5 obtained by direct measurements of protein concentration and fluorescence intensity, assuming no change in the quantum yield of 1,5-IAEDANS on reaction with 2-ITL-derivatized IF1.

The biologial activity of F-IF1 was tested in two assay systems. Its binding to 30S subunits was monitored by fluorescence intensity following sedimentation in sucrose density gradients. As shown in Figure 3, F-IF1 binds to the 30S subunit when IF2 and IF3 are included in the binding reaction but is not found in the 30S region of the gradient when the other factors are omitted. This dependence on IF2 and IF3 for IF1 binding to 30S subunits is consistent with earlier studies with [^{14}C]CH_3-IF1 (Langberg et al., 1977). The results show that F-IF1 is capable of specific factor-dependent binding to 30S subunits but do not indicate whether derivatization may have altered quantitative aspects of the interaction. A second assay employed was the stimulation of fMet-tRNA binding to 70S ribosomes in the presence of A-U-G and IF2 (Hershey et al., 1977). The activity of limiting amounts of this F-IF1 preparation was 90% of that for nonderivatized IF1. Since about 50% of the F-IF1 preparation is presumably unaltered, it is possible that the activities of F-IF1 derivatives are more impaired in this assay than the results above suggest. Nevertheless, it is clear that derivatization has not severely inactivated the F-IF1 and that the preparation is therefore suitable for more detailed studies.

Fluorescence Spectra and Lifetimes of F-IF1. A change in the quantum yield of F-IF1 upon binding to ribosomes would allow a relatively straightforward measure of the extent of binding of the factor. We therefore measured and compared the spectra of F-IF1 free and bound to 30S subunits. When excited at 337 nm, the corrected fluorescence emission spectrum of F-IF1 has a maximum at approximately 490 nm, similar to the emission from 1,5-IAEDANS in 60% ethanol (Hudson & Weber, 1973). Essentially no change in the intensity of emission and only a small shift to shorter wavelengths are seen on binding F-IF1 to 30S subunits in the presence of excess IF2 and IF3, after correcting for intrinsic fluorescence from 30S and the other factors (Figure 4). No significant

Table I: Fluorescent Lifetimes[a]

(A) Lifetimes[b]

		F-IF1 (ns)	F-IF1 + 30S (ns)	F-IF1 + 30S + IF2 + IF3 (ns)
6 MHz	τ_p	10.7 ± 0.7	15.5 ± 1.1	10.9 ± 0.8
	τ_m	12.2 ± 1.5	14.1 ± 1.5	14.4 ± 1.0
18 MHz	τ_p	10.1 ± 0.5	12.6 ± 0.9	7.9 ± 0.4
	τ_m	11.3 ± 1.2	14.9 ± 0.4	11.5 ± 2.0
30 MHz	τ_p	6.9 ± 0.9	10.3 ± 2.1	6.5 ± 0.4
	τ_m	9.9 ± 0.9	13.9 ± 2.2	9.8 ± 0.3

(B) Resolved Components[c]

	τ_1 (α_1)	τ_2 (α_2)	τ_1 (α_1)	τ_2 (α_2)	τ_1 (α_1)	τ_2 (α_2)
average	4 ± 2 (23 ± 15)	13 ± 5 (77 ± 15)	5 ± 4 (10 ± 7)	18 ± 3 (90 ± 7)	5 ± 1 (41 ± 5)	18 ± 4 (59 ± 5)
best fit	2.7 (17)	12.6 (83)	3.9 (10)	16.2 (90)	4.0 (39)	16.5 (61)

[a] Lifetimes for F-IF1 free or in 30S complexes were measured as described under Materials and Methods. [b] Lifetimes (in nanoseconds) at three frequencies. [c] Resolved components calculated either by weighted averages of components resolved from frequency pairs, or by a least squared error search best fit estimate from all three frequencies.

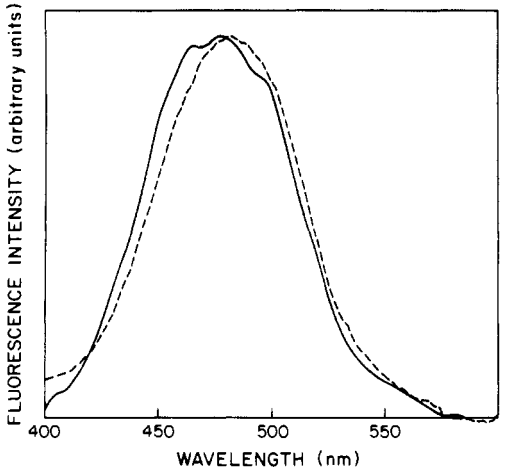

FIGURE 4: Spectra of bound and free fluorescent IF1. Samples in buffer B (100, 5) contained 150 nM free F-IF1 (---) or 150 nM F-IF1, 160 nM 30S subunits, 480 nM IF2, and 480 nM IF3 (—). Spectra were measured on the SLM 4800 with excitation wavelength at 337 nm, 16-nm excitation slit width, and 8-nm emission slit width. A glycogen reference was used to control for lamp fluctuation. Intrinsic fluorescence and scattering from 30S, IF2, and IF3 were measured and subtracted from the bound F-IF1 spectrum, and a five-point sliding regression analysis was applied to smooth the resulting difference spectrum.

difference was detected between free F-IF1 and F-IF1·30S, though interference from the high levels of 30S (≫1 μM) needed to bind F-IF1 in the absence of IF2 and IF3 was too strong to allow accurate interpretation of the F-IF1·30S emission spectrum (results not shown). We conclude that there is no significant difference in the quantum yield of F-IF1 in the free and bound states and therefore that we cannot use fluorescence intensity to measure F-IF1 binding.

An alternative approach to distinguishing bound and free F-IF1 is to measure fluorescence polarization, as was done in evaluating the ribosome binding of fluorescent derivatives of IF2 and IF3 (Weiel & Hershey, 1981, 1982). A change in polarization may reflect an altered rate of rotation of the probe and/or an altered lifetime of emission. Therefore, fluorescent lifetimes for free F-IF1, F-IF1·30S, and F-IF1·30S·IF2·IF3 were estimated by phase delay and fluorescence demodulation at three modulation frequencies as described under Materials and Methods. As shown in Table I, no single lifetime is consistent with all the observations for any of the three samples; at least two components with significant intensities must be present in each case. Heterogeneous components (t_1 and t_2) were resolved from data for pairs of frequencies (Weber, 1981), and the weighted averages from all three pairs are

Table II: Polarization of F-IF1 Bound to 30S[a]

	−IF3	+IF3
−IF2	0.11 ± 0.01	0.104 ± 0.006
+IF2	0.140 ± 0.002	0.181 ± 0.001

[a] P_b values for 30S·F-IF1 complexes with or without 300 nM excess of IF2 or IF3 over ribosomes were determined (Dandliker et al., 1964) by extrapolation to zero F-IF1 infinite 30S subunits.

reported. Alternatively, the two lifetimes were calculated by using data from all three frequencies at once, as described under Materials and Methods. Both methods of calculation give comparable results, namely, that free F-IF1 exhibits a minor component, t_1 (about 20% of emission), with a lifetime of about 3 ns and a major component, t_2 (about 80% of the emission), with a longer lifetime of about 13 ns (as will be discussed). As seen in Table I, both t_1 and t_2 are slightly shorter for free F-IF1 than for F-IF1 bound to 30S with or without IF2 and IF3. The small differences between free and bound F-IF1 are not expected to complicate interpretations of the polarization data described in the following section.

Polarization of F-IF1. The polarization of free F-IF1, P_f, was measured in buffer B (100, 5) in the absence of ribosomes and other initiation factors. The P_f values do not change over the concentration range 4–220 nM F-IF1; the weighted average of P_f is 0.042 ± 0.001. IF2 and IF3 have no effect on P_f, suggesting that under these conditions F-IF1 does not bind to other initiation factors in the absence of ribosomes. Next, the polarization of 100 mM F-IF1 was measured in the presence of an equimolar amount of 30S subunits. The polarization increases only slightly to about 0.06 (see Figure 5, open symbols at 0 factor add). However, when increasing amounts of one of the other initiation factor is added, P increases to about 0.10 with IF2 and to 0.08 with IF3 (Figure 5). The effects on P saturate at roughly 100 nM factor in both cases. Similar titrations, but in the presence of the third factor, also show an increase in P, with both curves saturating at P = 0.145. The increases in P could be due either to enhanced binding or to changes in the polarization of bound F-IF1 (P_b) caused by interactions of the factors with the fluorescent probe. The latter could occur only on the surface of the 30S subunit since IF2 and IF3 do not influence the P_f value in the absence of ribosomes.

We next measured the polarization of F-IF1 fully bound to 30S subunits (P_b), with or without a 300 nM excess of IF2 and IF3 over 30S subunits, using the double-extrapolation method of Dandliker et al. (1964). The P_b values reported in Table II are all significantly higher than P_f and are suitable for using polarization values to distinguish bound and free

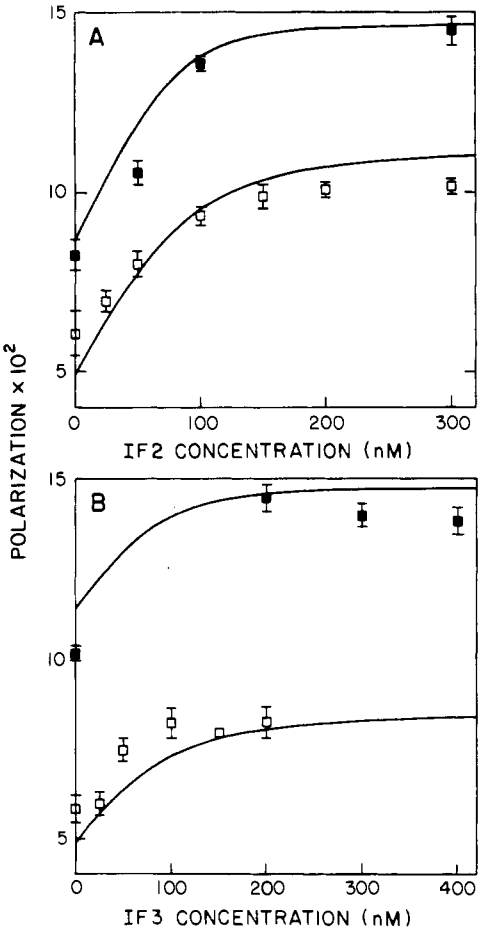

FIGURE 5: Effects of IF1 and IF3 on the polarization of F-IF1–30S subunit mixtures. Polarization was measured with samples in buffer B (100, 5) containing 100 nM F-IF1 and 100 nM 30S subunits. (Panel A) Samples also contained 200 nM IF3 (■) or no IF3 (□) with varying IF2. (Panel B) IF2 at 300 nM (■) or no IF2 (□) and IF3 as shown were added. Lines are theoretical polarization values based on P_f, P_b, and K_{af} from Tables II and III, assuming that IF2 binds to 30S subunits with an affinity of 5×10^7 M^{-1} in the presence of IF1, or 1×10^8 M^{-1} in the presence of IF1 and IF3 (Weiel & Hershey, 1982), and that IF3 binds with an affinity of 3.1×10^7 M^{-1} with or without other factors (Weiel & Hershey, 1981).

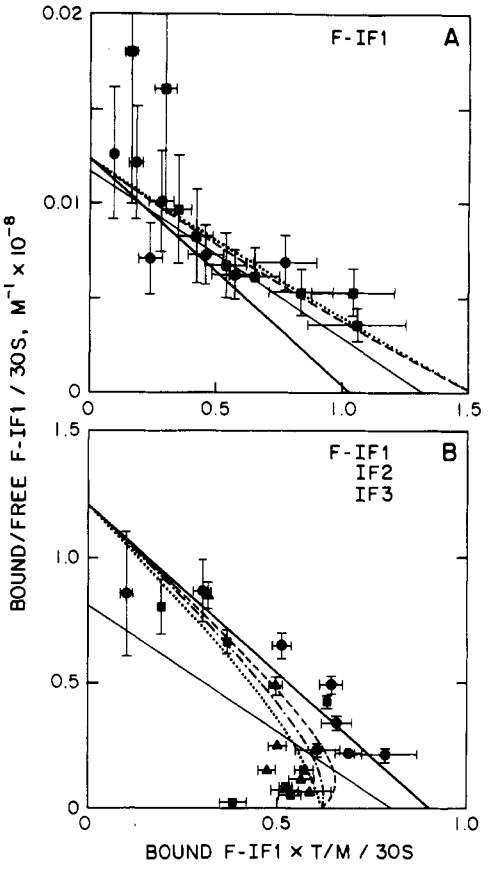

FIGURE 6: Scatchard plots of F-IF1 binding to 30S subunits. Polarization was measured from samples containing 30S subunits with (panel B) or without (panel A) IF2 and IF3 in 300 nM excess over 30S subunits, titrated with F-IF1. Bound/free F-IF1 ratios and bound F-IF1 were calculated from polarization and plotted according to eq 5b under Materials and Methods. Lines were fit by linear regression (model 1) using all points (—) or high B/F points only (—). Theoretical curves from model 2 (see text) are shown for each subunit concentration. (Panel A) 500 nM 30S (●) (···) or 1000 nM 30S (△) (- - -). (Panel B) 10 nM 30S (●) (···), 30 nM 30S (▲) (- · -) or 40 nM 30S (■) (- - -).

F-IF1.

Determination of Equilibrium Constants. Knowing P_f and P_b, and having shown that $Q_f/Q_b = 1$, we can calculate a bound/free ratio for F-IF1 from measured polarization (F_b/F_f) using eq 1 (see Materials and Methods). Increasing amounts of F-IF1 were titrated into mixtures of 30S subunits and factors as defined in the legend to Figure 6, and polarization was measured as described under Materials and Methods. Bound over free F-IF1 ratios calculated from these polarizations were plotted according to the modified Scatchard eq 5a as shown in Figure 6. The data were analyzed by using two different models. In model 1, it is assumed that the equilibrium association constant for nonderivatized IF1 (K_{an}) is equal to that for fluorescent-labeled IF1 (K_{af}). In model 2, K_{an} is not assumed to be equal to K_{af}. For model 1, points on a Scatchard plot should fit to a straight line, as in Figure 6A (solid line) with IF2 and IF3 absent from the titrations. In the presence of IF2 and IF3, we employed linear regression analysis of all the points to generate the solid line shown in Figure 6B. This gives a 30% error in the slope [$K_{af} = K_{an} = (1.0 \pm 0.3) \times 10^8$ M^{-1}], a stoichiometry (n) of 0.80 ± 0.06 F-IF1 sites per 30S subunits from the x axis intercept, and a residual error of 0.183 (i.e., the average difference between the model and the data is about 18%). Curvature to the left indicates that nonderivatized IF1 binds more tightly than F-IF1 and thereby reduces the amount of bound F-IF1 when IF1 and F-IF1 are in excess over 30S subunits. In other words, K_{an} appears to be larger than K_{af}.

Values for K_{an} and K_{af} were determined as described under Materials and Methods. Linear regression analysis of the portion of the data generated with relatively low amounts of added F-IF1 gives $K_{af} = (1.3 \pm 0.18) \times 10^8$ M^{-1} from the slope and $n = 0.90 \pm 0.03$ from the intercept (Figure 6B, dashed line). Competition between IF1 and F-IF1 at high IF1 to 30S ratios was then analyzed by using this K_{af} value to calculate N_b/N_f according to eq 9 and plotting this ratio vs. F_b/F_f according to eq 4. The slope of the line that fits these points and passes through the origin is $K_{af}/K_{an} = 0.53 \pm 0.06$. This ratio of affinities is consistent with data from competition experiments where the ratio of fluorescent to nonfluorescent IF1 was varied by mixing nonderivatized IF1 with the F-IF1 preparation (results not shown). K_{af} was then divided by this ratio to calculate $K_{an} = (2.5 \pm 0.45) \times 10^8$ M^{-1}. The predicted F_b/F_f vs. F_b curves, with $K_{af} = 1.3 \times 10^8$ M^{-1}, $K_{an} = 2.5 \times 10^8$ M^{-1}, and $n = 0.90$, fit the data substantially better than the first model, giving a residual error of only 0.103 (curved lines, Figure 6B). Thus, IF1 binds to 30S·IF2·IF3 roughly twice as well as F-IF1.

When the K_{af} to K_{an} ratio was used to recalculate N_b for adjusted Scatchard plots as described under Materials and

Table III: IF1 Association Constants and Stoichiometry[a]

IF2	IF3	model	IF1 association constant K_{an} (M^{-1})	IF1 sites per 30S	residual error	relative affinity K_{af}/K_{an}
−	−	1	$9 \pm 1 \times 10^5$	1.32 ± 0.09	0.169	
		2	$5 \pm 1 \times 10^5$	1.0 ± 0.1	0.181	3.6 ± 0.5
−	+	1	$4.6 \pm 0.6 \times 10^7$	1.39 ± 0.06	0.132	
		2	$3.6 \pm 0.4 \times 10^7$	1[b]	0.152	2.4 ± 0.1
+	−	1	$9 \pm 1 \times 10^7$	0.93 ± 0.04	0.101	
		2	$1.1 \pm 0.2 \times 10^8$	0.99 ± 0.04	0.107	0.86 ± 0.08
+	+	1	$1.0 \pm 0.3 \times 10^8$	0.80 ± 0.06	0.183	
		2	$2.5 \pm 0.5 \times 10^8$	0.90 ± 0.03	0.103	0.53 ● 0.06

[a] Association constants and stoichiometries were calculated for IF1·30S complexes as described under Materials and Methods and Results. Data analyses by models 1 ($K_{af} = K_{an}$) and 2 ($K_{af} \neq K_{an}$) are given under Materials and Methods. [b] K_{af} was determined from a dissociation plot (Glaser et al., 1982). [30S]/[Bound/free F-IF1] vs. [30S]/([30S] − [bound F-IF1]) assuming one site per subunit; the slope of a line through the origin fitted to data points with high B/F yields $K_d = 1/K_a$.

Methods, no significant change was seen in points with high F_b/F_f, confirming that the first approximation of K_{af} was valid. Cycles of adjusted Scatchard and competition plots using all points converged on $K_{af} = (1.4 \pm 0.12) \times 10^8$ M^{-1}, $n = 0.96 \pm 0.02$, $K_{af}/K_{an} = 0.42 \pm 0.05$, and $K_{an} = (3.4 \pm 0.49) \times 10^8$ M^{-1} with a residual error of 0.088. These adjusted values fit the data slightly better but are not significantly different from the original estimates.

Similar analyses were performed on the data obtained from titrations in the absence of IF2 and IF3 (Figure 6A) and with either IF2 or IF3 present (data not shown). Values for K_{af} and K_{an} were calculated with both models and are reported in Table III. There is good agreement for the K_{an} values between the two models except for the binding reaction containing IF2 and IF3. Table III shows clearly the influence of IF2 and IF3 on IF1 binding. In the absence of the other factors, IF1 binding is very weak. IF3 alone causes about a 50-fold increase in the binding constant whereas IF2 alone stimulates it 100–200-fold. With the two factors together, the K_a is increased up to 500-fold. There is a single IF1 binding site on the 30S subunit when IF2 is present, but in the absence of IF2, IF1, or at least F-IF1, may bind at more than one site.

Effects of Mono- and Divalent Cations on F-IF1 Binding. Physiological salt conditions may affect IF1 binding in vivo, so the effects of ammonium and magnesium ions on F-IF1 and IF1 binding to 30S subunits were examined. No significant changes in P_f, P_b, Q_f/Q_b, or K_{af}/K_{an} were detected in the ranges of 50–150 mM NH_4Cl or 2.5–10 mM $Mg(OAc)_2$. Magnesium has a relatively small effect on F-IF1 binding: a plot of log K_a vs. log $[Mg^{2+}]$ has a slope of -0.54 ± 0.07, and the ratios of the K_a's at 2.5, 5, and 10 mM $Mg(OAc)_2$ are 1.6:1.0:0.6 (data not shown). Ammonium has a much stronger effect: log K_a vs. log $[NH_4^+]$ has a slope of -2.6 ± 0.3; at 50, 100, and 150 mM NH_4Cl, the ratios of the K_a's are 4.5:1.0:0.23 (data not shown). K_{an} for IF1 depends heavily on the presence of other initiation factors on the subunit (see above), and IF2 binding is sensitive to salt (Weiel & Hershey, 1982); therefore, it is necessary to control for reduced IF2 binding at high salt. IF2 was increased in concentration to overcome its decreased affinity. At 150 mM NH_4Cl, the K_a for IF2 drops to roughly 9×10^6 M^{-1} (Weiel & Hershey, 1982). Therefore, IF2 was raised from 0.3 μM excess to 5 μM excess to saturate 90% of the subunits at this low affinity; IF3 was also raised to 0.5 μM excess to counteract its slight salt sensitivity. Under these conditions, F-IF1 had an affinity for 30S of $(0.5–3) \times 10^7$ M^{-1} at 150 mM NH_4Cl, considerably weaker than the K_{af} of 1×10^8 M^{-1} observed at 100 mM NH_4Cl. When IF2 was omitted, F-IF1 binding to 30S in buffer B (150, 5) was difficult to detect; K_{af} was at most 1×10^6 M^{-1}, far less than the K_{af} of at least 4×10^7 M^{-1} seen in 100 mM salt. Thus, experiments with either extra IF2 or no IF2 confirm that NH_4^+ affects F-IF1 binding directly, though an additional indirect effect through IF2 is not ruled out.

Discussion

We have prepared covalent fluorescent derivatives of IF1 in order to measure the equilibrium binding constant of the factor with the 30S ribosomal subunit using fluorescence polarization. Inactivation of IF1 by acylation was avoided by treating the protein with 2-iminothiolane and IAEDANS. The F-IF1 preparation contains on the average about 0.6 dansyl group per factor, with very few factor molecules possessing more than two fluorescent groups (Figure 2). This heterologous population of dansyl derivatives retains biological activity. F-IF1 binds stably to 30S subunits in the presence of IF2 and IF3 (Figure 3) and promotes fMet-tRNA binding to 70S ribosomes. The effect of derivatization on IF1 binding was evaluated quantitatively from the polarization data. The method enables us to calculate the K_a's for both nonderivatized IF1 and for the F-IF1 population (Table III). F-IF1 binds about 2.5-fold more tightly than IF1 to 30S subunits in the absence of IF2. In the presence of IF2, this relationship is reversed, and nonderivatized IF1 binds nearly 2-fold more tightly than F-IF1. The different binding affinities calculated for the F-IF1 molecules reflect an average of possibly different values for each molecular species present. No attempt has been made to evaluate the relative contributions of the many expected monoderivatized species or of the species carrying two dansyl groups.

Little or no change in the intensity of fluorescence occurs on binding F-IF1 to 30S subunits. Therefore, fluorescence polarization techniques were used to measure the extent of F-IF1 binding at equilibrium, as has been done previously with F-IF2 and F-IF3 (Weiel & Hershey, 1981, 1982). The difference in polarization between free and ribosome-bound F-IF1 is 0.068–0.139, depending on the binding mixture, and is sufficient to calculate association constants. The rise in polarization on binding to ribosomes is due primarily to an increase in the rotational relaxation time rather than to substantial changes in fluorescence lifetimes (Table I).

IF1 binds only weakly to 30S subunits in the absence of the other initiation factors ($K_a \leq 10^6$ M^{-1}). Addition of IF3 enhances the affinity about 50-fold and IF2, about 150-fold. When both IF2 and IF3 are present, the affinity of IF1 increases up to 500-fold ($K_a = 2.5 \times 10^8$ M^{-1}). The strong enhancement of IF1 binding by the other initiation factors previously has been observed qualitatively by measuring the binding of $[^{14}C]CH_3$-IF1 to 30S subunits by sucrose gradient centrifugation (Langberg et al., 1977). The weak binding interaction of IF1 with 30S subunits reported by Gualerzi and Pon (1981) is consistent with our quantitative results, whereas the IF1 binding described by Van der Hofstad and co-workers

(1978) cannot be readily evaluated or compared because glutaraldehyde fixation was employed. In addition to being influenced by the presence of the other initiation factors, the K_a for IF1 is very sensitive to ionic strength but less so to Mg^{2+} at $\leq$10 mM concentration. Similar behavior was observed for IF2 (Weiel & Hershey, 1982), whereas the affinity of IF3 for 30S subunits is not greatly altered by either monovalent or divalent cations (Weiel & Hershey, 1981).

The changes in K_a, P_b, and fluorescence lifetimes observed when IF2 and/or IF3 are included in the binding mixtures provide some insight into the interaction of all three factors on the surface of the 30S subunit. Besides the large increase in K_a, the addition of IF2 causes P_b to rise from 0.110 to 0.140. The increase in P_b is not likely due to a change in the rotational relaxation time of the whole complex but rather suggests that IF2 influences the mobility of the dansyl probe in its microenvironment. The presence of IF2 also results in quantitative differences in the binding constants for derivatized (K_{af}) and nonderivatized (K_{an}) IF1, consistent with a direct interaction with IF1 on the ribosome. In contrast, IF3 causes no significant change in P_b nor does it alter the K_{af}:K_{an} ratio (Table III), which suggests that IF3 might not bind adjacent to IF1. The results reported here are consistent with the structural model for initiation factor binding to 30S subunits based on cross-linking studies (Boileau et al., 1983), where IF2 binds contiguously to IF1 and IF3, but the latter two factors appear not to be in direct contact.

In previous papers we reported that the affinity of IF2 for 30S subunits is increased about 3-fold by IF1 and IF3 (Weiel & Hershey, 1982) while that for IF3 is not affected by other factors (Weiel & Hershey, 1981). Here we show that IF2 and IF3 cause increases in the K_a for IF1 of roughly 150- and 50-fold, respectively. Each of these studies was performed under equilibrium conditions. At each point in the titrations, measurements were repeated until P was stable, indicating that the binding reactions had reached apparent equilibrium. Also, in each study the same apparent equilibrium was approached from several directions by adding the fluorescent initiation factor before (e.g., Figure 5) or after (e.g., Figure 6) the other factors. However, the combined data are not consistent with a simple equilibrium model of factor binding:

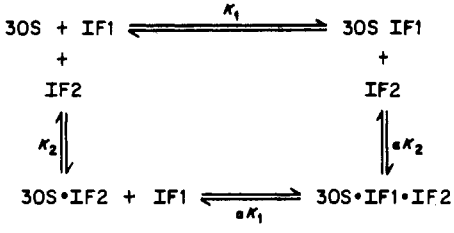

This model predicts that the effect of IF1 on IF2 binding (less than 3-fold) should be equal to the effect of IF2 on IF1, but the latter is 2 orders of magnitude greater than the former. Similarly, IF3 binding increases the K_a's for both IF1 and IF2, but the converse is not found. These results are more consistent with a class of models that include a conformational change in the 30S subunit:

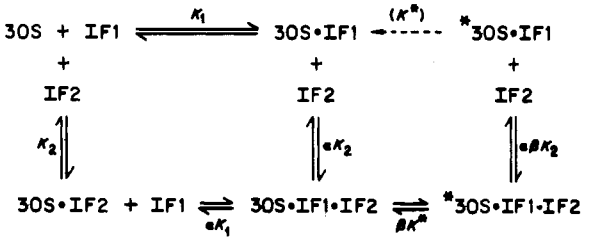

where *30S is the new subunit conformation. This conformation can be reached when IF1 and IF2 are bound to the subunit, but not when IF1 alone is bound. IF2 can bind to and dissociate from *30S·IF1, but IF1 cannot be released from the new conformation without returning to the original state: IF1 may be trapped in a pocket that only closes in the presence of IF2. This model fits the observed data if the product $\alpha\beta$ is about 2 and K^* is about 100. The gradual increase in polarization seen on adding IF2 to a mixture of F-IF1 and 30S subunits (Figure 5A) may be due to an irreversible conversion of *30S·IF1 directly to 30S·IF1 (dashed arrow in the diagram). Without this step, addition of substoichiometric amounts of IF2 would catalyze the convfersion of 30S·IF1 to *30S·IF1 through 30S·IF1·IF2 and *30S·IF1·IF2. This would result in an abrupt 100-fold increase in the apparent K_a for IF1, which is not consistent with the results shown in Figure 5 assuming P_b for *30S·IF1 is at least as high as that for 30S·IF1. Therefore, the results suggest that a steady state is reached at low IF2. At saturating IF2 we observe a true equilibrium where 30S·IF2 and *30S·IF1·IF2 are the major species; the constant K_a is equal to $\alpha\beta K^* K_1$ in the above diagram.

Analogous models are consistent with the data for interactions of IF3 with IF1 or IF2 on the 30S subunit, e.g., substitute IF3 for IF2 in the model above. IF3-induced conformational changes in 30S subunits have been detected by physical and chemical methods (Pon et al., 1982). Similar techniques may provide evidence for conformational changes induced by combinations of initiation factors as proposed here. Additional polarization experiments such as F-IF1 titrations into solutions of 30S subunits with substoichiometric IF2 or IF3 would also be useful to test these models, especially with stopped-flow measurements of kinetic rate constants.

The association constants measured for IF1, IF2, and IF3 indicate that all three factors should essentially saturate their binding sites on the native 30S subunit in the intact *E. coli* cell. The concentration of 70S ribosomes in the cell is about 10 μM; since native ribosomal subunits represent about 10% of the total ribosomes, and the initiation factor to ribosome ratio is about 0.2 (Howe & Hershey, 1981), their concentrations are about 1–2 μM. Using the $K_a = 2.5 \times 10^8$ M^{-1} in buffer B (100, 5), we calculate that greater than 98% of the IF1 binding sites on 30S subunits will contain IF1. If the intracellular ionic strength is comparable to buffer B (200, 5) instead, extrapolation of the data on salt concentration effects gives a $K_a = 5 \times 10^6$, which is still sufficient to saturate about 70% of the IF1 binding sites. It is therefore reasonable to conclude that native 30S subunits contain IF1 as well as other initiation factors. Work is in progress to determine the association constants for each of the initiation factors in other initiation complexes proposed for the pathway of initiation.

ACKNOWLEDGMENTS

We thank Dr. Jurgen Weiel for preparations of purified IF2 and IF3 and Dorothy Derania for expert typing.

Registry No. 1,5-IAEDANS, 36930-63-9; 2-ITL hydrochloride, 4781-83-3; NH_4^+, 14798-03-9.

REFERENCES

Dandliker, W. B., Shapiro, H. C., Meduiski, J. W., Alonso, R., Feigen, G. A., & Hamrick, J. R., Jr. (1964) *Immunochemistry 1*, 165–191.

Ellis, S., & Conway, T. W. (1984) *J. Biol. Chem. 259*, 6707–7614.

Fakunding, J. L., & Hershey, J. W. B. (1973) *J. Biol. Chem. 248*, 4206–4212.

Glaser, C. B., Broderick, J. W., Dreschel, D., Karic, L., Grececeffo, M., & Largman, C. (1982) *Biochemistry 21*, 556–561.
Grunberg-Manago, M., Buckingham, R. H., Cooperman, B. S., & Hershey, J. W. B. (1978) *Symp. Soc. Gen. Microbiol. 28th*, 27–110.
Gualerzi, C., & Pon, C. L. (1981) *Struct. Aspects Recognit. Assemb. Biol. Macromol., Proc. Aharon Katzir-Katchalsky Conf., 7th*, 805–826.
Gualerzi, C., Risuleo, G., & Pon, C. L. (1977) *Biochemistry 16*, 1684–1689.
Heimark, R. L., Hershey, J. W. B., & Traut, R. R. (1976) *J. Biol. Chem. 251*, 7779–7784.
Hershey, J. W. B., Yanov, J., Johnston, K., & Fakunding, J. L. (1977) *Arch. Biochem. Biophys. 182*, 626–638.
Hudson, E. N., & Weber, G. (1973) *Biochemistry 12*, 4154–4161.
Laemmli, U. K. (1970) *Nature (London) 227*, 680–685.
Langberg, S. R., Kahan, L., Traut, R. R., & Hershey, J. W. B. (1977) *J. Mol. Biol. 117*, 307–319.
Maitra, U., Stringer, E. A., & Chaudhuri, A. (1982) *Annu. Rev. Biochem. 51*, 869–900.
Maizel, J. V., Jr. (1971) *Methods Virol 5*, 179–246.
Matthews, H. (1984) in *A Laboratory Manual of Methods in Molecular Biology* (Walker, J. M., Ed.) Humana Press, Clifton, NJ.
O'Farrell, P. Z., Goodman, H. M., & O'Farrell, P. H. (1977) *Cell (Cambridge, Mass.) 12*, 1133–1142.
Pon, C. L., Pawlik, R. T., & Gualerzi, C. (1982) *FEBS Lett. 137*, 163–167.
Scatchard, C. (1949) *Ann. N.Y. Acad. Sci. 51*, 660–672.
Schaffner, W., & Weissmann, C. (1973) *Anal. Biochem. 56*, 502–514.
Spencer, R. D., & Weber, G. (1973) *Ann. N.Y. Acad. Sci. 158*, 361–376.
Van der Hofstad, G. A. J. M., Buitenhek, A., Bosch, L., & Voorma, H. O. (1978) *Eur. J. Biochem. 89*, 213–220.
Weber, G. (1981) *J. Phys. Chem. 85*, 949–953.
Weiel, J., & Hershey, J. W. B. (1981) *Biochemistry 20*, 5859–5865.
Weiel, J., & Hershey, J. W. B. (1982) *J. Biol. Chem. 257*, 1215–1220.
Wintermeyer, W., & Gualerzi, C. (1983) *Biochemistry 22*, 690–694.
Worthing, A. G., & Geffner, J. (1949) *Treatment of Experimental Data*, Wiley, New York.
Zamir, A., Miskin, R., & Elson, D. (1971) *J. Mol. Biol. 60*, 347–364.

Magnesium Ion Dependent Equilibria, Kinetics, and Thermodynamic Parameters of *Artemia* Ribosome Dissociation and Subunit Association†

Dixie J. Goss* and Terry Harrigan

Department of Chemistry, Hunter College of the City University of New York, New York, New York 10021

Received August 6, 1985; Revised Manuscript Received February 24, 1986

ABSTRACT: The influence of magnesium ion concentration on the equilibrium and kinetics of *Artemia* ribosome dissociation and subunit association has been studied by laser light scattering. Ribosomal aggregation was found to be reduced by addition of 0.1–0.05 mM spermidine and KCl concentrations of 100 mM. The ribosomes were found to be stable at low [Mg^{2+}], and the curves obtained for ribosome–subunit equilibrium were independent of the direction and origin of the magnesium ion titration. Thermodynamic parameters were obtained from the temperature-dependent equilibria and have been compared to those of wheat germ and *Escherichia coli* type A ribosomes. The entropy term calculated for the association of 40S and 60S subunits is small, and the reaction is exothermic. The entropy term is negative, favoring subunit dissociation, and contributes less to the free energy than the enthalpy term. Rate constants for ribosome dissociation and subunit association have been determined. The reaction curves gave no evidence for sequential processes and were homogeneous.

The reversible association and dissociation of ribosomal subunits play a central role in the process of protein biosynthesis in both eucaryotes and procaryotes. The ion-dependent association and dissociation equilibrium and kinetics of procaryotic *Escherichia coli* ribosomal subunits have been extensively studied, but there is less data available for eucaryotic ribosomes. Some procaryotic protein biosynthesis is greater than an order of magnitude faster than eucaryotic protein biosynthesis, kinetic and thermodynamic studies are of particular interest in understanding the differences between protein synthesis in eucaryotes and procaryotes. The effects of a variety of cations on the equilibrium of eucaryotic wheat germ ribosomal subunits with 80S monosomes has been explored (Sperrazza et al., 1980, 1981; Sperrazza & Spremulli, 1983; Moore & Spremulli, 1985), but no kinetic data were reported. Physicochemical studies have been carried out on *Artemia* (brine shrimp) ribosomes (Nieuwenhuysen & Clauwaert, 1981; Nieuwenhuysen et al., 1981; Donceel et al., 1982). Electron microscopy (Lake et al., 1974; Boublik & Hellman, 1978) and other physical techniques (Nieuwenhuysen & Clauwaert, 1981; Nieuwenhuysen et al., 1980) suggested

† This work was supported in part by funds from Research Corporation and the City University of New York PSC–CUNY Research Award Program.

* Author to whom correspondence should be addressed.

0006-2960/86/0425-3690$01.50/0